

Article

Efficient and Eco-Friendly Perspectives for C-H Arylation of Benzothiazole Utilizing Pd Nanoparticle-Decorated Chitosan

Mohamed Mokhtar M. Mostafa ^{1,*}, Tamer S. Saleh ², Salem M. Bawaked ¹, Khadijah S. Alghamdi ³
and Katabathini Narasimharao ^{1,*}

¹ Chemistry Department, Faculty of Science, King Abdulaziz University, P.O. Box 80203, Jeddah 21589, Saudi Arabia

² Chemistry Department, Faculty of Science, University of Jeddah, P.O. Box 80329, Jeddah 21589, Saudi Arabia

³ Chemistry Department, Faculty of Science, Al-Baha University, Albaha 65779, Saudi Arabia

* Correspondence: mmoustafa@kau.edu.sa (M.M.M.M.); nkatabathini@kau.edu.sa (K.N.)

Abstract: In this contribution, an eco-friendly, sustainable, and efficient palladium nanoparticle-decorated chitosan (Pd@Chitosan) catalyst was synthesized by a simple impregnation method. The synthesized material was utilized as a heterogeneous catalyst for the C-H arylation of benzothiazole under ultrasonic irradiation. The Pd@Chitosan catalyst efficiently catalyzed the conversion of aryl iodides and bromides to 1-(4-(benzothiazol-2-yl)phenyl)ethan-1-one selectively. A single product of 83–93% yield was obtained in *N,N*-dimethylformamide solvent at 80 °C for 2.5h. This study reveals that Pd@Chitosan is an efficient catalyst, which catalyzes the C-H arylation with good reaction yields. The activity of the Pd@Chitosan is due to the presence of highly dispersed Pd(0) nanoparticles on the surface of the chitosan and Pd²⁺; a tentative mechanism was proposed based on the XPS results of the fresh catalyst and spent catalyst.

Keywords: Pd@Chitosan; C-H arylation; 2-aryl benzothiazole; ultrasound irradiation



Citation: Mostafa, M.M.M.; Saleh, T.S.; Bawaked, S.M.; Alghamdi, K.S.; Narasimharao, K. Efficient and Eco-Friendly Perspectives for C-H Arylation of Benzothiazole Utilizing Pd Nanoparticle-Decorated Chitosan. *Catalysts* **2022**, *12*, 1000. <https://doi.org/10.3390/catal12091000>

Academic Editor: Victorio Cadierno

Received: 4 August 2022

Accepted: 30 August 2022

Published: 5 September 2022

Publisher's Note: MDPI stays neutral with regard to jurisdictional claims in published maps and institutional affiliations.



Copyright: © 2022 by the authors. Licensee MDPI, Basel, Switzerland. This article is an open access article distributed under the terms and conditions of the Creative Commons Attribution (CC BY) license (<https://creativecommons.org/licenses/by/4.0/>).

1. Introduction

The circular economy is gradually replacing linear economies, thereby ensuring that consumer materials and chemical elements are recycled efficiently in the future. With this paradigm shift, we aim to preserve the needs of future generations in terms of energy consumption, safe and comfortable materials, and sustainable access to raw and renewable feedstocks [1,2]. Of note, the interest in the utilization of metal nanoparticles as catalysts for organic synthesis has increased considerably because of their high efficiency under environmentally benign reaction conditions [3]. Continuous efforts are ongoing to develop effective and eco-friendly noble metal-based catalysts, although there are many drawbacks observed in the utilization of these catalysts, such as self-agglomeration and the leaching of metal nanoparticles, which negatively affect the catalytic or recycling performance [4–7]. The choice of an ideal support is one of the major ways to avoid the mentioned drawbacks. The selected support should have a high surface area and specific chelating functional groups to strongly interact with the metal nanoparticles [8,9]. Many different inorganic and organic supports have been used to immobilize various metal nanoparticles [10–12]. Among the bio-based organic supports, natural polysaccharides are the most investigated due to their specific properties such as an eco-friendly nature, large surface area, nontoxicity, high chelating capacity, etc. [13,14]. Chitosan, a natural polysaccharide, is of particular interest for utilization in catalysis due to its suitability as an excellent catalyst support [15–21]. In addition, its insolubility in organic solvents makes it attractive in developing heterogeneous catalysts [22,23]. Due to these outstanding properties, chitosan could be excellent support and a stabilizer to decorate with active metal nanoparticles.

Great interest has been observed in the synthetic chemistry community for the direct functionalization of C-H bonds via supported transition-metal catalysts as a powerful

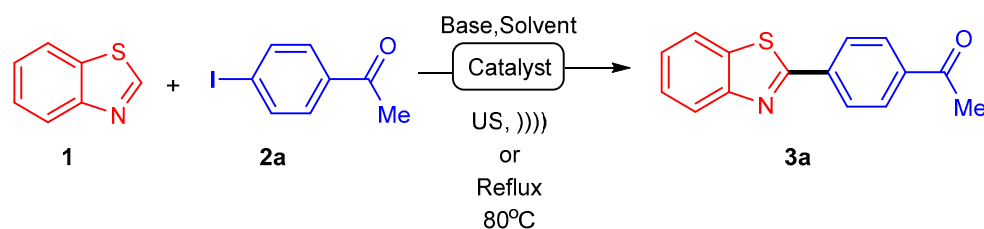
and practical alternative to the well-applied Pd catalyzed cross-coupling reactions to avoid the prefunctionalization of the starting materials [24–27], in addition to many recent reports dealing with C-H functionalization utilizing different green chemistry tools [28–30]. However, some limitations have been realized for the synthetic utility of the direct C-H arylation processes, such as the selective functionalization among multiple C-H bonds in the reactant substrates [31]. It is preferable to use electronically activated substrates such as heteroaromatics to overcome these drawbacks. In addition, benzothiazole derivatives are an essential class of compounds used for synthesizing pharmacophore intermediates. For instance, 2-Arylbenzothiazoles can be effectively used as synthetic building blocks for anticancer [32,33], anti-hepatitis C virus (anti-HCV) [34], antioxidant, and anti-glutamic acid drug molecules [35].

Ultrasound irradiation is widely used along with heterogeneous catalysts to synthesize different organic compounds. It has been used with a catalyst for C-H arylation of benzothiazole. Using ultrasound accelerates the synthesis of organic compounds and saves the energy required for the reactions [36,37]. Thus, in continuation of our interest in the green synthesis of biologically active heterocyclic compounds [38–45], herein, we have fabricated fully characterized palladium nanoparticle-decorated chitosan.

2. Results and Discussion

2.1. C-H Arylation of Benzothiazole

We initiated our study with the reaction of benzothiazole (**1**) and 4-iodo acetophenone (**2a**) (Scheme 1). This reaction, illustrated in Scheme 1, was taken as a model reaction to optimize the reaction conditions (Table 1).



Scheme 1. Optimization of the reaction conditions for the C-H arylation reaction of benzothiazole.

A palladium nanoparticle-decorated chitosan (Pd@chitosan) catalyst (0.05 g) was tested. Initially, the reaction between equimolar amounts of benzothiazole (**1**) and 4-iodoacetophenone (**2a**) (2 mmol) in the presence of potassium carbonate as base (one equiv.) and catalyst under ultrasonic conditions was performed, and we obtained the target product identified as 1-(4-(benzothiazol-2-yl)phenyl)ethan-1-one (**3a**) as a sole product at an 81% yield in *N,N*-dimethylformamide (DMF) at 80 °C for 3 h (Table 1, entry 3).

Next, we increased the amount of the catalyst to 0.1g with the same molar ratio and the conditions mentioned above. There was no change after increasing the amount of catalyst (Table 1, entry4). The rising amount of potassium carbonate to two equivalent was beneficial for the reaction to be smoothly conducted, reducing the time to 2.5 h at an 83% yield under ultrasonic irradiation (Table 1, entry 5). When the reaction was conducted with three equivalent of potassium carbonate, no further improvement in the yield was noticed (Table 1, entry 6). Next, we screened different solvents. Acetonitrile (ACN), dimethyl sulfoxide (DMSO), dichloromethane (DCM), and tetrahydrofuran (THF) were used under the same abovementioned scale in the presence of the Pd@chitosan catalyst and potassium carbonate at a temperature of 80 °C. The results showed that DMF was the best solvent, as a yield of 83% of **3a** was obtained (entry 5 and entries 7–10). Then, we screened different bases such as potassium acetate, sodium carbonate, and potassium phosphate; no large difference was noticed, and potassium carbonate remained the most effective (entries 11–13).

Table 1. The reaction conditions for Pd@Chitosan catalysis of the C-H arylation of benzothiazole.

Entry	Base (Equiv.)	Catalyst	Solvent	Ultrasound Irradiation ^a		Silent Condition ^a	
				Yield ^b (%)	Time (h)	Yield ^b (%)	Time (h)
1	K ₂ CO ₃ (1)	None	DMF	-	-	-	-
2	K ₂ CO ₃ (1)	Chitosan	DMF	-	-	-	-
3	K ₂ CO ₃ (1)	5%Pd@Chitosan (0.05 g)	DMF	81	3.0	48	16
4	K ₂ CO ₃ (1)	5%Pd@Chitosan (0.1 g)	DMF	81	3.0	48	16
5	K ₂ CO ₃ (2)	5%Pd@Chitosan (0.05 g)	DMF	83	2.5	51	16
6	K ₂ CO ₃ (3)	5%Pd@Chitosan (0.05 g)	DMF	83	2.5	51	16
7	K ₂ CO ₃ (2)	5%Pd@Chitosan (0.05 g)	ACN	59	4.0	38	24
8	K ₂ CO ₃ (2)	5%Pd@Chitosan (0.05 g)	DMSO	43	5.5	33	24
9	K ₂ CO ₃ (2)	5%Pd@Chitosan (0.05 g)	DCM	26	6.0	17	36
10	K ₂ CO ₃ (2)	5%Pd@Chitosan (0.05 g)	THF	41	5.5	33	24
11	CH ₃ COOK (2)	5%Pd@Chitosan (0.05 g)	DMF	81	3.0	50	16
12	Na ₂ CO ₃ (2)	5%Pd@Chitosan (0.05 g)	DMF	80	3.0	50	16
13	K ₃ PO ₄ (2)	5%Pd@Chitosan (0.05 g)	DMF	79	3.0	50	16

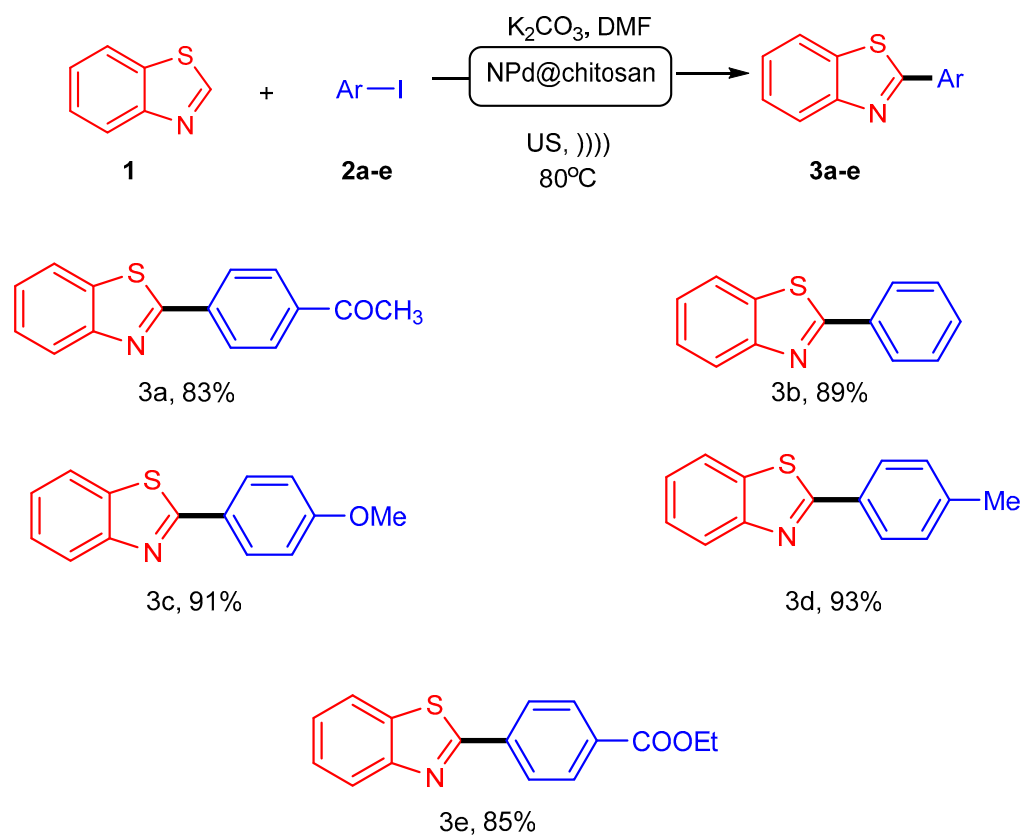
^a Reaction conditions: equimolar amounts of benzothiazole (1) and 4-iodoacetophenone (2a) in the presence of two equivalent of potassium carbonate in DMF (10 mL) at 80 °C under ultrasonic irradiation and/or silent conditions. ^b The % yield calculated in each time for the obtained crude products.

Of note, under ultrasonic irradiation, no product formed in the absence of the catalyst (entry 1) or in the presence of the chitosan (catalyst support) (entry 2).

To find the beneficial effect of the ultrasound on this reaction, all the reactions were carried out under conventional reaction conditions without ultrasound irradiation (Table 1). However, it was observed that under the traditional reaction conditions, the yield of the products decreased, and the reactions required significantly longer periods. Thus, ultrasound was found to have an influence on the C-H arylation reaction in the present methodology.

The effect of halogen in the used aryl halide also was tested; for example, in the above model reaction, we used 4-bromoacetophenone instead of the 4-iodoacetophenone (**2a**) under the same optimized reaction conditions, and no obvious effect was noticed as almost same reaction yield and time were attained for the product **3a**. The apparent effect of the ultrasound irradiation on the abovementioned reaction over the silent condition can be interpreted in light of the micro-jet impact and shockwave damage at the liquid–solid interface [46]. Along with the shock wave associated with the cavitation collapse, the jet caused localized deformation and surface erosion, which increased the possible reaction area. Therefore, the treated surfaces contained increased dislocations that are widely considered active sites in catalysis [46,47]. The cavitation intensity rises depending on the type of solvent and frequency used. As we work at a constant frequency of 37 kHz, the solvent used to perform the sonochemical reaction must be carefully chosen. Any particles or motes (solid catalysts) present in the solvent will act as seeds for cavitation [45]. As a general rule, most sonochemical applications are performed in water. However, in our reaction case, we used DMF. It was found that DMF had the nearest viscosity to water at 70–80 °C [48], and cavitation is easier in solvents with low viscosities [45]. The above facts led us to interpret the observed reactivity for our reaction under ultrasound over silent conditions and the superiority of DMF over other tested solvents.

The scope and generality of the present methodology were tested by synthesizing benzothiazole derivatives using Pd@chitosan catalyst under the optimized reaction conditions (Scheme 2). The products **3a–e** were obtained in good yields (83–93%) (Scheme 2). All the obtained structures in Scheme 2 provided satisfactory elemental analysis and spectroscopic data (see the experimental section).



Scheme 2. The scope of the C-H arylation of benzothiazole and the structure of 2-arylbenzothiazoles using Pd@chitosan catalyst under the optimized conditions.

2.2. Catalyst Characterization

X-Ray Photoelectron Spectroscopy (XPS)

The deconvoluted XPS spectra for the fresh and spent Pd@Chitosan samples are shown in Figure 1. Both the fresh and spent catalyst samples exhibited two Pd $3d$ core peaks indicating the presence of Pd species with two different oxidation states. The contributions corresponding to Pd $3d_{5/2}$ at 341.0 eV and Pd $3d_{3/2}$ at 346.2 eV indicated the presence of Pd(II) species [49]. In addition, there were minor contributions due to the presence of Pd(0) species with its binding energy at 337.4 eV and 343.1 eV, respectively [50]. In the spent catalyst, the presence of similar Pd species with lower binding energies were observed, due to the different chemical nature of the neighboring atoms on an individual surface. It is also known that the binding energy varies with the change in shielding effect [51]. The spent catalyst was characterized by an increase in the proportion of the Pd (0) species (increased from 45 to 50%). The reduction of Pd can be explained by the presence of solvents and the reaction conditions used for C-H arylation. The C $1s$ spectra for fresh and spent Pd@Chitosan samples had three peaks in the range of 284.7 eV to 289.4 eV. The peaks observed at 285.1 eV, 286.6 eV, and 289.4 eV could be assigned to the C-C/C=C, C=N, and O-C=O functional groups, respectively [52]. The high intensity of the peaks in the fresh sample compared to the spent sample confirmed the strong network consisting of carbon and nitrogen bonds. The contribution due to the peak at 286.8 eV was predominant in the case of the spent catalyst, and this was possibly due to presence of C=N groups in the benzothiazole molecules adsorbed on the surface of the spent catalyst.

The deconvoluted N $1s$ spectra for both samples are shown in Figure 1. The fresh sample exhibited three different N $1s$ deconvoluted peaks with a binding energy of 399.4 eV corresponding to $-NH_2$ or $-NH$ of chitosan, 401 eV to C=N, and 402.7 eV to the Pd bonded to $-NH$ or $-NH_2$ groups [41]. However, the spent catalyst showed the presence of a low intensity peak due to the Pd bonded to the $-NH_2/-NH$ functional groups of chitosan; the decrease in the intensity of this peak was possibly due to the leaching of some Pd species from the chitosan surface during the reaction. The presence of different N $1s$ peaks in different chitosan samples was previously observed, and it was due to the change in the chemistry of the chitosan material (different sources and functional groups, etc.) [53]. The fresh Pd@Chitosan sample exhibited O $1s$ peaks at 532.5 eV and 534.0 eV, which could be assigned to the oxygen species of the N-C=O and C-OH/C-O-C in the chitosan structure, respectively [54]. The third peak at a higher binding energy (536.5 eV) could be attributed to the Pd bonded oxygen containing carbon species [55]. The spent catalyst also showed three O $1s$ peaks; however, the binding energy of the XPS peaks was shifted to lower levels due to the change in the shielding effect. Interestingly, the intensity of the peak at 532.5 eV due to the N-C=O species was increased in the case of the spent catalyst, which was due to the C=N bonds of the benzothiazole molecule.

2.3. Tentative Mechanism

It is reasonable to propose a mechanism for the C-H arylation of benzothiazole under the adopted reaction conditions (Scheme 3). Based on the characterization of the fresh and the spent catalysts, a possible reaction mechanism for the arylation of benzothiazole is depicted in Scheme 3. The proposed catalytic cycle based on the Pd in our catalyst present as Pd(II) in the majority may involve the following steps: (i) palladation of benzothiazole via C-H activation as indicated from the XPS in which the presence of the peak at 286.8 eV was predominant in case of the spent catalyst, which may be due to the presence of the C=N groups in the benzothiazole molecules, indicating the possible Pd adsorbed or coordinated on the surface of the spent catalyst; (ii) the oxidation addition of aryl iodide and formation of Pd(III) cannot be excluded [56,57], as well as Pd(IV) [58]; and the (iii) reductive elimination affording monoarylated product **3** as exclusive product, and the Pd(II) in addition to some Pd(IV) or Pd (III) may be reduced to Pd (0), as indicated from the XPS in which the spent catalyst was characterized by a slight increase in the proportion of the Pd (0) species (increasing from 45 to 50%).

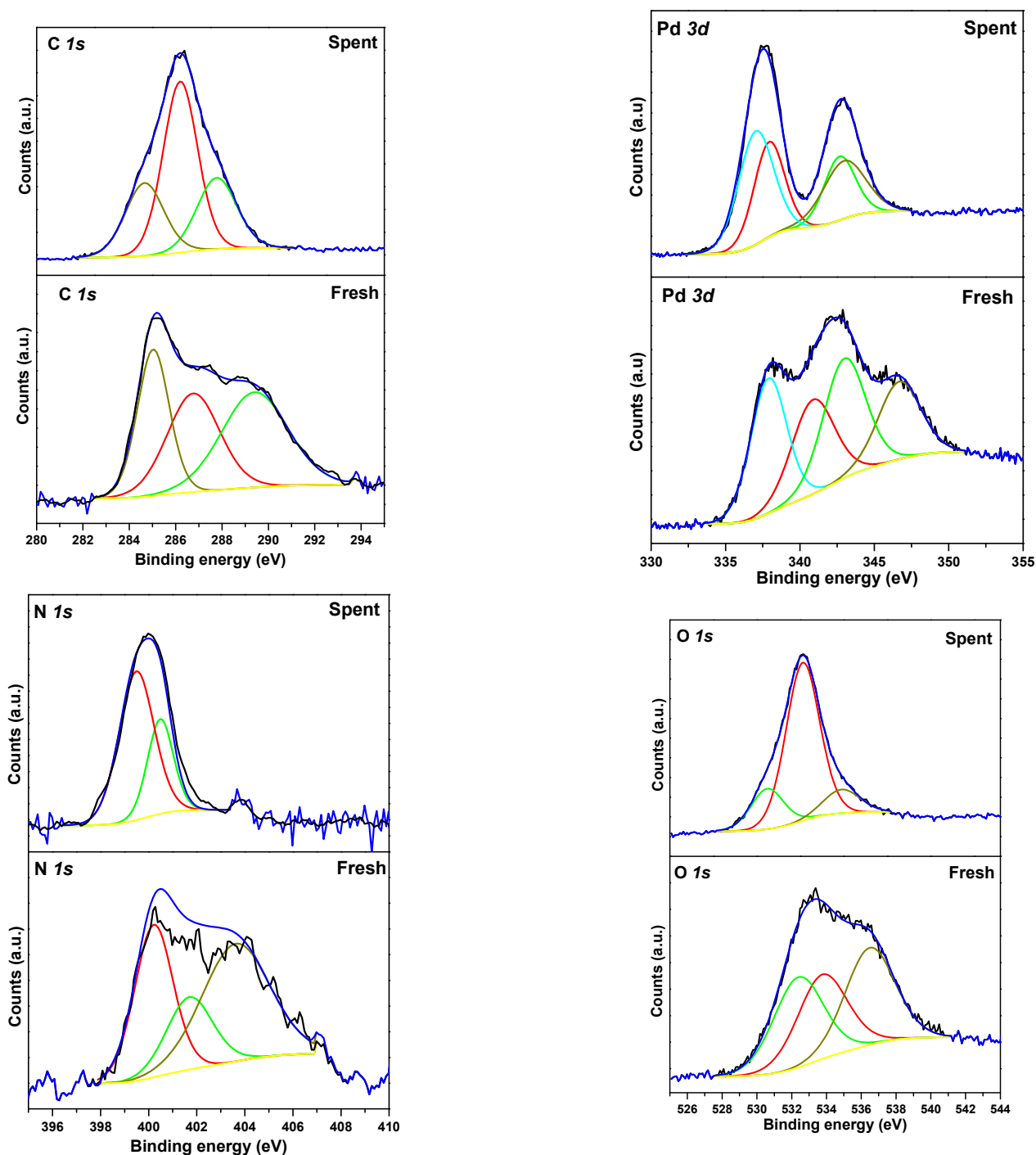
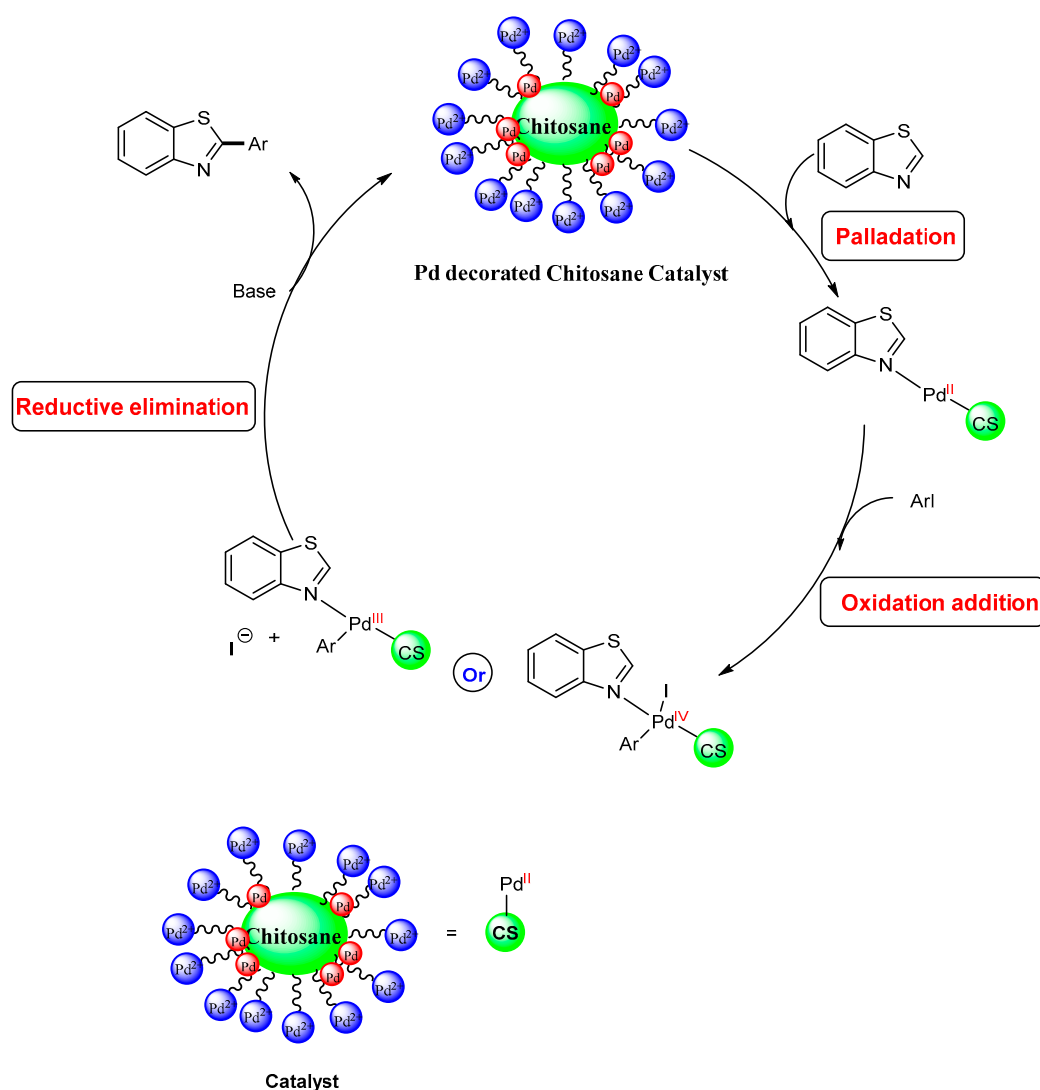


Figure 1. XPS spectra for the fresh and spent Pd@Chitosan samples.

We cannot ignore that the reaction may have been through Pd(0) to certain extent, which began with the oxidative addition of aryl halide to form $\text{Ar-Pd}^{\text{II}}\text{-X}$, followed by transmetalation enhanced by the base present to form benzothiazole (BT)- $\text{Pd}^{\text{II}}\text{-Ar}$, and finally by reductive elimination, it may have formed the BT-Ar and the regenerated catalyst. However, in our opinion, the first mechanism is more acceptable based on the XPS data.

Of note, we used the spent catalyst for a new run for the CH arylation reaction to study the recyclability of the catalyst; we obtained the product **3a** in same yield and time for the second run. However, in the third run, there was no product obtained even after six hours, which means leaching of Pd may have occurred.



Scheme 3. Tentative mechanism of Pd@chitosan catalyst for CH arylation of benzothiazole.

3. Experiments

3.1. Reagents

All the chemicals used in this work were of high analytical grades, including chitosan (molecular weight 100,000–300,000) (Acros Organics, Geel, Belgium) and palladium (II) acetate (Sigma Aldrich, Bangalore, India). All organic chemicals were purchased from Acros Organics (Geel, Belgium) and used as is without further purification.

Thin-layer chromatography (TLC) was performed on pre-coated Merck 60 GF254 silica gel plates with a fluorescent indicator and detection utilizing UV light at 254 and 360 nm. The melting points were measured on a Stuart melting point apparatus and were uncorrected. IR spectra were recorded on a Smart iTR, an ultrahigh-performance versatile Attenuated Total Reflectance (ATR) sampling accessory on the Nicolet iS10 FT-IR (Thermo Scientific, Waltham, MA, USA) spectrometer. The NMR spectra were recorded on a Bruker Avance III 400 (Bruker, Billerica, MA, USA) (9.4 T, 400.13 MHz for ^1H , 100.62 MHz for ^{13}C) spectrometer with a 5-mm BBFO probe, at 298 K, and a Bruker High Performance Digital FT-NMR Spectrometer Avance III 850 MHz. Chemical shifts (δ in ppm) were given relative to the internal solvent, DMSO- d_6 2.50 for ^1H and 39.50 for ^{13}C ; CDCl_3 7.25 for ^1H and 77.7 was used as an external standard. Mass spectra were recorded on a Thermo ISQ Single Quadrupole GC-MS (Waltham, MA, USA). Elemental analyses were carried out on a Euro Vector instrument C, H, N, S analyzer EA3000 Series (Pavia, Italy). Sonication was

performed by the Techno-gaz sonicator (with a frequency of 37 kHz and ultrasonic peak max. 320 W).

3.2. Synthesis of Pd Nanoparticle-decorated Chitosan Sample (5% Pd@chitosan)

The synthesis of constant Pd nanoparticles conducted with chitosan as a natural polymer with steady properties and the absence of toxicity in a one-step process, following the method described by Manikandan and Muthukrishnan [59]. First, 0.75 g chitosan was dissolved in 100 mL 0.1% acetic acid (in distilled water). Then, 25 mL of 0.015 M palladium solution was added to 50 mL of the chitosan solution under stirring at 70 °C for 9 h until the reaction was completed. The colloid was centrifuged for 10 min. to separate particles from suspension and washed with acetone (90%, *v/v*); the centrifugation was repeated three times to remove unreacted reagents. The cake was then dried under vacuum at room temperature overnight and stored.

3.3. C-H arylation of Benzothiazole

3.3.1. Silent Reactions

In 10 mL DMF, potassium carbonate (1mmol) was added and stirred for 30 min. Then a mixture of benzothiazole (1) (0.5 mmol), different aryl halides (0.5 mmol), and Pd catalyst (0.05 g) were added, and the mixture was refluxed at 80 °C for the appropriate time (Table 1) until completion of the reaction (monitored by TLC). The reaction mixture was filtered to separate the catalyst; then, the filtrate was cooled at room temperature, and the reliable product obtained was filtered, dried, and purified by recrystallization from ethanol.

3.3.2. Sonicated Reactions

These processes were performed on the same scale described above for the silent reactions. All the reactions were kept at 80 °C, which was attained by adding or removing water in an ultrasonic bath (the temperature inside the reaction vessel was 74–76 °C). The sonochemical reactions were continued for a suitable time (Table 1) until the starting materials were no longer detectable by TLC. Then, the catalyst was separated, and the products obtained were purified as described above in the silent reaction procedures. The synthesized compounds with their physical data are depicted in the Supplemental Information. We washed the spent catalyst with hot ethyl acetate and sonicated for 5 min. to desorb all adsorbed product on their surface; this was followed by filtration and drying prior to a new catalytic test.

4. Conclusions

We introduced an efficient sustainable heterogeneous catalyst based on a natural polymer and minimal loading of Pd for selective C-H monoarylation of benzothiazole in high yields and short reaction times utilizing ultrasound irradiations. A tentative mechanism was suggested for this reaction based on the XPS of the fresh and spent catalyst after the first run.

Supplementary Materials: The following supporting information can be downloaded at: <https://www.mdpi.com/article/10.3390/catal12091000/s1>, Figure S1. Powder XRD; Figure S2. DR UV-vis; Figure S3. H₂-TPR of Pd@Chitosan sample; Figure S4. The physical and spectroscopic data of the synthesized compounds; Figure S5. NMR Charts of the synthesized compounds.

Author Contributions: Writing—review and editing, M.M.M.M. and T.S.S.; writing—review and editing, M.M.M.M. and K.N.; project administration, M.M.M.M.; funding acquisition, M.M.M.M.; supervision, S.M.B.; formal analysis, K.S.A.; investigation, S.M.B. and K.S.A.; data curation, T.S.S. and K.N. All authors have read and agreed to the published version of the manuscript.

Funding: Deanship of Scientific Research (DSR) at King Abdulaziz University, Jeddah under grant no. G:163-130-1440.

Data Availability Statement: The data presented in this study are available in supplementary materials.

Acknowledgments: This project was funded by the Deanship of Scientific Research (DSR) at King Abdulaziz University, Jeddah under grant no. G:163-130-1440. The authors, therefore, acknowledge with thanks DSR for technical and financial support.

Conflicts of Interest: The authors claim that they do not have any known conflicting financial interests or personal affiliations that may seem to have impacted the work presented in this study.

References

1. Keijer, T.; Bakker, V.; Sloopweg, J.C. Circular Chemistry to enable a Circular Economy. *Nat. Chem.* **2019**, *11*, 190–195.
2. Zuin, V.G.; Kümmerer, K. Chemistry and Materials Science for a Sustainable Circular Polymeric Economy. *Nat. Rev. Mater.* **2022**, *7*, 76–78.
3. Hemmati, S.; Heravi, M.M.; Karmakar, B.; Veisi, H. Green Fabrication of Reduced Graphene Oxide Decorated with Ag Nanoparticles (RGO/Ag NPs) Nanocomposite: A Reusable Catalyst for the Degradation of Environmental Pollutants in Aqueous Medium. *J. Mol. Liq.* **2020**, *319*. [[CrossRef](#)]
4. García-Suárez, E.J.; Lara, P.; García, A.B.; Ojeda, M.; Luque, R.; Philippot, K. Efficient and Recyclable Carbon-Supported Pd Nanocatalysts for the Suzuki-Miyaura Reaction in Aqueous-Based Media: Microwave vs Conventional Heating. *Appl. Catal. A Gen.* **2013**, *468*, 59–67. [[CrossRef](#)]
5. Fu, Y.; Xu, P.; Huang, D.; Zeng, G.; Lai, C.; Qin, L.; Li, B.; He, J.; Yi, H.; Cheng, M.; et al. Au Nanoparticles Decorated on Activated Coke via a Facile Preparation for Efficient Catalytic Reduction of Nitrophenols and Azo Dyes. *Appl. Surf. Sci.* **2019**, *473*, 578–588. [[CrossRef](#)]
6. Nasri, A.; Jaleh, B.; Nezafat, Z.; Nasrollahzadeh, M.; Azizian, S.; Jang, H.W.; Shokouhimehr, M. Fabrication of G-C₃N₄/Au Nanocomposite Using Laser Ablation and Its Application as an Effective Catalyst in the Reduction of Organic Pollutants in Water. *Ceram. Int.* **2021**, *47*, 3565–3572. [[CrossRef](#)]
7. Zeynizadeh, B.; Rahmani, S.; Tizhoush, H. The Immobilized Cu Nanoparticles on Magnetic Montmorillonite (MMT@Fe₃O₄@Cu): As an Efficient and Reusable Nanocatalyst for Reduction and Reductive-Acetylation of Nitroarenes with NaBH₄. *Polyhedron* **2020**, *175*, 114201. [[CrossRef](#)]
8. Veisi, H.; Najafi, S.; Hemmati, S. Pd(II)/Pd(0) Anchored to Magnetic Nanoparticles (Fe₃O₄) Modified with Biguanidine-Chitosan Polymer as a Novel Nanocatalyst for Suzuki-Miyaura Coupling Reactions. *Int. J. Biol. Macromol.* **2018**, *113*, 186–194. [[CrossRef](#)]
9. Ahmad, P.T.; Jaleh, B.; Nasrollahzadeh, M.; Issaabadi, Z. Efficient Reduction of Waste Water Pollution Using GO/γMnO₂/Pd Nanocomposite as a Highly Stable and Recoverable Catalyst. *Sep. Purif. Technol.* **2019**, *225*, 33–40. [[CrossRef](#)]
10. Ei-Shobaky, G.A.; Abroad, A.S.; Mokhtar, M. Effect of Gamma-Irradiation on Surface and Catalytic Properties of CuO-ZnO/Al₂O₃ System. *J. Radioanal. Nucl. Chem.* **1997**, *219*, 89–94.
11. Mokhtar, M.; Ohlinger, C.; Schlander, J.H.; Turek, T. Hydrogenolysis of Dimethyl Maleate on Cu/ZnO/Al₂O₃ Catalysts. *Chem. Eng. Technol.* **2001**, *24*, 423–426.
12. Veisi, H.; Hamelian, M.; Hemmati, S. Palladium Anchored to SBA-15 Functionalized with Melamine-Pyridine Groups as a Novel and Efficient Heterogeneous Nanocatalyst for Suzuki-Miyaura Coupling Reactions. *J. Mol. Catal. A Chem.* **2014**, *395*, 25–33. [[CrossRef](#)]
13. Nasrollahzadeh, M.; Sajjadi, M.; Iravani, S.; Varma, R.S. Starch, Cellulose, Pectin, Gum, Alginate, Chitin and Chitosan Derived (Nano)Materials for Sustainable Water Treatment: A Review. *Carbohydr. Polym.* **2021**, *251*, 116986.
14. Jamwal, N.; Sodhi, R.K.; Gupta, P.; Paul, S. Nano Pd(0) Supported on Cellulose: A Highly Efficient and Recyclable Heterogeneous Catalyst for the Suzuki Coupling and Aerobic Oxidation of Benzyl Alcohols under Liquid Phase Catalysis. *Int. J. Biol. Macromol.* **2011**, *49*, 930–935. [[CrossRef](#)]
15. Kumar, M.N.V.R. A Review of Chitin and Chitosan Applications. *React. Funct. Polym.* **2000**, *46*, 1–27.
16. Ma, J.; Sahai, Y. Chitosan Biopolymer for Fuel Cell Applications. *Carbohydr. Polym.* **2013**, *92*, 955–975.
17. Pillai, C.K.S.; Paul, W.; Sharma, C.P. Chitin and Chitosan Polymers: Chemistry, Solubility and Fiber Formation. *Prog. Polym. Sci.* **2009**, *34*, 641–678.
18. Baig, R.B.N.; Nadagouda, M.N.; Varma, R.S. Ruthenium on Chitosan: A Recyclable Heterogeneous Catalyst for Aqueous Hydration of Nitriles to Amides. *Green Chem.* **2014**, *16*, 2122–2127. [[CrossRef](#)]
19. Guibal, E. Heterogeneous Catalysis on Chitosan-Based Materials: A Review. *Prog. Polym. Sci.* **2005**, *30*, 71–109.
20. Guibal, E. Interactions of Metal Ions with Chitosan-Based Sorbents: A Review. *Sep. Purif. Technol.* **2004**, *38*, 43–74. [[CrossRef](#)]
21. Sun, J.; Wang, J.; Cheng, W.; Zhang, J.; Li, X.; Zhang, S.; She, Y. Chitosan Functionalized Ionic Liquid as a Recyclable Biopolymer-Supported Catalyst for Cycloaddition of CO₂. *Green Chem.* **2012**, *14*, 654–660. [[CrossRef](#)]
22. Chtchigrovsky, M.; Primo, A.; Gonzalez, P.; Molvinger, K.; Robitzer, M.; Quignard, F.; Taran, F. Functionalized Chitosan as a Green, Recyclable, Biopolymer-Supported Catalyst for the [3+2] Huisgen Cycloaddition. *Angew. Chem. Int. Ed.* **2009**, *48*, 5916–5920. [[CrossRef](#)]
23. Kumar, S.; Singhal, N.; Singh, R.K.; Gupta, P.; Singh, R.; Jain, S.L. Dual Catalysis with Magnetic Chitosan: Direct Synthesis of Cyclic Carbonates from Olefins with Carbon Dioxide Using Isobutyraldehyde as the Sacrificial Reductant. *Dalton Trans.* **2015**, *44*, 11860–11866. [[CrossRef](#)]

24. Alberico, D.; Scott, M.E.; Lautens, M. Aryl-Aryl Bond Formation by Transition-Metal-Catalyzed Direct Arylation. *Chem. Rev.* **2007**, *107*, 174–238.
25. Lewis, J.C.; Bergman, R.G.; Ellman, J.A. Direct Functionalization of Nitrogen Heterocycles via Rh-Catalyzed C-H Bond Activation. *Acc. Chem. Res.* **2008**, *41*, 1013–1025. [[CrossRef](#)]
26. Amii, H.; Uneyama, K. C-F Bond Activation in Organic Synthesis. *Chem. Rev.* **2009**, *109*, 2119–2183. [[CrossRef](#)]
27. Chen, X.; Engle, K.M.; Wang, D.H.; Yu, J.Q. Palladium(II)-Catalyzed C-H Activation/C-C Cross-Coupling Reactions: Versatility and Practicality. *Angew. Chem. Int. Ed.* **2009**, *48*, 5094–5115.
28. Das, D.; Bhutia, Z.T.; Chatterjee, A.; Banerjee, M. Mechanochemical Pd(II)-Catalyzed Direct and C-2-Selective Arylation of Indoles. *J. Org. Chem.* **2019**, *84*, 10764–10774.
29. Albano, G.; Decandia, G.; Capozzi, M.A.M.; Zappimulso, N.; Punzi, A.; Farinola, G.M. Infrared Irradiation-Assisted Solvent-Free Pd-Catalyzed (Hetero)aryl-aryl Coupling via C–H Bond Activation. *ChemSusChem* **2021**, *14*, 3391–3401.
30. Sharma, A.; Vacchani, D.; Van der Eycken, E. Developments in direct C-H arylation of (hetero)arenes under microwave irradiation. *Chemistry* **2013**, *19*, 1158–1168. [[CrossRef](#)]
31. Liu, X.W.; Shi, J.L.; Yan, J.X.; Wei, J.B.; Peng, K.; Dai, L.; Li, C.G.; Wang, B.Q.; Shi, Z.J. Regioselective Arylation of Thiazole Derivatives at 5-Position via Pd Catalysis under Ligand-Free Conditions. *Org. Lett.* **2013**, *15*, 5774–5777. [[CrossRef](#)]
32. Gong, B.; Hong, F.; Kohm, C.; Bonham, L.; Klein, P. Synthesis and SAR of 2-Arylbenzoxazoles, Benzothiazoles and Benzimidazoles as Inhibitors of Lysophosphatidic Acid Acyltransferase- β . *Bioorganic Med. Chem. Lett.* **2004**, *14*, 1455–1459. [[CrossRef](#)]
33. Mortimer, C.G.; Wells, G.; Crochard, J.P.; Stone, E.L.; Bradshaw, T.D.; Stevens, M.F.G.; Westwell, A.D. Antitumor Benzothiazoles. 26.1 2-(3,4-Dimethoxyphenyl)-5-Fluorobenzothiazole (GW 610, NSC 721648), a Simple Fluorinated 2-Arylbenzothiazole, Shows Potent and Selective Inhibitory Activity against Lung, Colon, and Breast Cancer Cell Lines. *J. Med. Chem.* **2006**, *49*, 179–185. [[CrossRef](#)]
34. Wee Phoon, C.; Yong Ng, P.; Ting, A.E.; Ling Yeo, S.; Mui Sim, M. Biological Evaluation of Hepatitis C Virus Helicase Inhibitors. *Bioorganic Med. Chem. Lett.* **2001**, *11*, 1647–1650.
35. Benazzouz, A.; Boraud, T.; Dube, P. dat, A. Boireau, J.-M. Stutzmann, C. Gross. *Eur. J. Pharmacol.* **1995**, *284*, 10–16.
36. Mokhtar, M.; Alhashedi, B.F.A.; Kashmery, H.A.; Ahmed, N.S.; Saleh, T.S.; Narasimharao, K. Highly Efficient Nanosized Mesoporous CuMgAl Ternary Oxide Catalyst for Nitro-Alcohol Synthesis: Ultrasound-Assisted Sustainable Green Perspective for the Henry Reaction. *ACS Omega* **2020**, *5*, 6532–6544. [[CrossRef](#)]
37. Saleh, T.S.; Al-Bogami, A.S.; Mekky, A.E.M.; Alkhathlan, H.Z. Sonochemical Synthesis of Novel Pyrano [3,4-e] [1,3] Oxazines: A Green Protocol. *Ultrason. Sonochemistry* **2017**, *36*, 474–480. [[CrossRef](#)]
38. Saleh, T.S.; Narasimharao, K.; Ahmed, N.S.; Basahel, S.N.; Al-Thabaiti, S.A.; Mokhtar, M. Mg-Al Hydrotalcite as an Efficient Catalyst for Microwave Assisted Regioselective 1,3-Dipolar Cycloaddition of Nitrilimines with the Enaminone Derivatives: A Green Protocol. *J. Mol. Catal. A Chem.* **2013**, *367*, 12–22. [[CrossRef](#)]
39. Narasimharao, K.; Al-Sabban, E.; Saleh, T.S.; Gallastegui, A.G.; Sanfiz, A.C.; Basahel, S.; Al-Thabaiti, S.; Alyoubi, A.; Obaid, A.; Mokhtar, M. Microwave Assisted Efficient Protocol for the Classic Ullmann Homocoupling Reaction Using Cu-Mg-Al Hydrotalcite Catalysts. *J. Mol. Catal. A Chem.* **2013**, *379*, 152–162. [[CrossRef](#)]
40. Bassyouni, F.A.; Saleh, T.S.; Elhefnawi, M.M.; El-Moez, S.I.A.; El-Senousy, W.M.; Abdel-Rehim, M.E. Synthesis, Pharmacological Activity Evaluation and Molecular Modeling of New Polynuclear Heterocyclic Compounds Containing Benzimidazole Derivatives. *Arch. Pharmacol. Res.* **2012**, *35*, 2063–2075. [[CrossRef](#)]
41. Shahid, A.; Ahmed, N.S.; Saleh, T.S.; Al-Thabaiti, S.A.; Basahel, S.N.; Schwieger, W.; Mokhtar, M. Solvent-Free Biginelli Reactions Catalyzed by Hierarchical Zeolite Utilizing a Ball Mill Technique: A Green Sustainable Process. *Catalysts* **2017**, *7*, 84. [[CrossRef](#)]
42. Mady, M.F.; Saleh, T.S.; El-Kateb, A.A.; Abd El-Rahman, N.M.; Abd El-Moez, S.I. Microwave-Assisted Synthesis of Novel Pyrazole and Pyrazolo [3,4-d] Pyridazine Derivatives Incorporating Diaryl Sulfone Moiety as Potential Antimicrobial Agents. *Res. Chem. Intermed.* **2016**, *42*, 753–769. [[CrossRef](#)]
43. Al-Bogami, A.S.; Saleh, T.S.; Mekky, A.E.M.; Shaaban, M.R. Microwave Assisted Regioselective Synthesis and 2D-NMR Studies of Novel Azoles and Azoloazines Utilizing Fluorine-Containing Building Blocks. *J. Mol. Struct.* **2016**, *1121*, 167–179. [[CrossRef](#)]
44. El Maksod, I.H.A.; Saleh, T.S. The Use of Nano Supported Nickel Catalyst in Reduction of P-Nitrophenol Using Hydrazine as Hydrogen Donor. *Green Chem. Lett. Rev.* **2010**, *3*, 127–134. [[CrossRef](#)]
45. Ahmed, N.S.; Menzel, R.; Wang, Y.; Garcia-Gallastegui, A.; Bawaked, S.M.; Obaid, A.Y.; Basahel, S.N.; Mokhtar, M. Graphene-Oxide-Supported CuAl and CoAl Layered Double Hydroxides as Enhanced Catalysts for Carbon-Carbon Coupling via Ullmann Reaction. *J. Solid State Chem.* **2017**, *246*, 130–137. [[CrossRef](#)]
46. Mason, T.J. The design of ultrasonic reactors for environmental remediation. In *Ultrasound in Environmental Protection*; Elsevier: Amsterdam, The Netherlands, 2001; pp. 247–268.
47. Shah, Y.T.; Pandit, A.B.; Moholkar, V.S. *Cavitation Reaction Engineering*; Springer Science & Business Media: Berlin, Germany, 1999.
48. Gmehling, J. N, N-Dimethylformamide (DMF) Dynamic Viscosity: Datasheet from “Dortmund Data Bank (DDB)—Thermophysical Properties Edition 2014” in SpringerMaterials; Springer-Verlag Berlin Heidelberg & DDBST GmbH: Oldenburg, Germany. Available online: https://materials.springer.com/thermophysical/docs/vis_c72 (accessed on 4 August 2022).
49. Shaikh, N.; Pamidimukkala, P. Magnetic Chitosan Stabilized Palladium Nanostructures: Potential Catalysts for Aqueous Suzuki Coupling Reactions. *Int. J. Biol. Macromol.* **2021**, *183*, 1560–1573. [[CrossRef](#)]

50. Tsyurul'nikov, P.G.; Afonasenkov, T.N.; Koshcheev, S.V.; Boronin, A.I. State of Palladium in Palladium-Aluminosilicate Catalysts as Studied by XPS and the Catalytic Activity of the Catalysts in the Deep Oxidation of Methane. *Kinet. Catal.* **2007**, *48*, 728–734. [[CrossRef](#)]
51. Amaral, I.F.; Granja, P.L.; Barbosa, M.A. Chemical Modification of Chitosan by Phosphorylation: An XPS, FT-IR and SEM Study. *J. Biomater. Sci. Polym. Ed.* **2005**, *16*, 1575–1593. [[CrossRef](#)]
52. Balakrishnan, A.; Appunni, S.; Gopalram, K. Immobilized TiO₂/Chitosan Beads for Photocatalytic Degradation of 2,4-Dichlorophenoxyacetic Acid. *Int. J. Biol. Macromol.* **2020**, *161*, 282–291. [[CrossRef](#)]
53. Dong, Y.; Bi, J.; Ming, S.; Zhang, S.; Zhu, D.; Meng, D.; Li, T. Functionalized Chitosan as a Novel Support for Stabilizing Palladium in Suzuki Reactions. *Carbohydr. Polym.* **2021**, *260*, 117815. [[CrossRef](#)]
54. Luo, M.; Wang, X.; Meng, T.; Yang, P.; Zhu, Z.; Min, H.; Chen, M.; Chen, W.; Zhou, X. Rapid One-Step Preparation of Hierarchical Porous Carbon from Chitosan-Based Hydrogel for High-Rate Supercapacitors: The Effect of Gelling Agent Concentration. *Int. J. Biol. Macromol.* **2020**, *146*, 453–461. [[CrossRef](#)]
55. Kumari, S.; Layek, S.; Pathak, D.D. Palladium Nanoparticles Immobilized on a Magnetic Chitosan-Anchored Schiff Base: Applications in Suzuki-Miyaura and Heck-Mizoroki Coupling Reactions. *New J. Chem.* **2017**, *41*, 5595–5604. [[CrossRef](#)]
56. Powers, D.C.; Geibel, M.A.L.; Klein, J.E.M.N.; Ritter, T. Bimetallic Palladium Catalysis: Direct Observation of Pd(III)-Pd(III) Intermediates. *J. Am. Chem. Soc.* **2009**, *131*, 17050–17051. [[CrossRef](#)]
57. Mc Glacken, G.P.; Bateman, L.M. Recent Advances in Aryl–Aryl Bond Formation by Direct Arylation. *Chem. Soc. Rev.* **2009**, *38*, 2447–2464. [[CrossRef](#)]
58. Ding, Q.; Ji, H.; Wang, D.; Lin, Y.; Yu, W.; Peng, Y. Pd(II)-Catalyzed Ortho Arylation of 2-Arylbenzothiazoles with Aryl Iodides via Benzothiazole-Directed C-H Activation. *J. Organomet. Chem.* **2012**, *711*, 62–67. [[CrossRef](#)]
59. Muthukrishnan, A.M. Green Synthesis of Copper-Chitosan Nanoparticles and Study of Its Antibacterial Activity. *J. Nanomed. Nanotechnol.* **2015**, *6*, 1000251. [[CrossRef](#)]